A Design of the Low-Pass Filter Using the Novel Microstrip Defected Ground Structure

Dal Ahn, *Member, IEEE*, Jun-Seok Park, *Associate Member, IEEE*, Chul-Soo Kim, *Student Member, IEEE*, Juno Kim, *Student Member, IEEE*, Yongxi Qian, *Member, IEEE*, and Tatsuo Itoh, *Life Fellow, IEEE*

***Abstract*—A new defected ground structure (DGS) for the microstrip line is proposed in this paper. The proposed DGS unit structure can provide the bandgap characteristic in some frequency bands with only one or more unit lattices. The equivalent circuit for the proposed defected ground unit structure is derived by means of three-dimensional field analysis methods. The equivalent-circuit parameters are extracted by using a simple circuit analysis method. By employing the extracted parameters and circuit analysis theory, the bandgap effect for the provided defected ground unit structure can be explained. By using the derived and extracted equivalent circuit and parameter, the low-pass filters are designed and implemented. The experimental results show excellent agreements with theoretical results and the validity of the modeling method for the proposed defected ground unit structure.**

***Index Terms*—Bandgap, defected ground structure, equivalent circuit, low-pass filter.**

I. Introduction

A DEFECTED ground structure (DGS) for the microstrip line, such as various microstrip photonic bandgap (PBG) structures, which have periodic etched defects in backside metallic ground plane, is one of the most interesting areas of research. The PBG research was done in the optical fields originally, but the PBG structures can be applied to wide frequency ranges, including the microwave frequency band by properly scaled dimension. Recently, there has been an increasing interest in microwave and millimeter-wave applications of PBG circuits. [1]–[3] The only PBG structures, which have a periodic structure, have been known as providing rejection of certain frequency bands, i.e., bandgap effect. [4]–[8] Many passive and active microwave and millimeter devices have been developed to suppress the harmonics and realize the compact physical dimensions of circuits. Several efforts have been made to realize such devices on a various PBG circuits—e.g., a power amplifier with PBG circuits [9], [10], the PBG structure for slow-wave circuits [11], and realization of a magnetic wall in waveguide [12], [13]; their experimental results are sufficient to show the validity of PBG circuit applications. However, it is difficult to use a PBG structure for the design of the microwave or millimeter-wave components due to the difficulties of the modeling. There are too many design parameters, which have an affect on the bandgap property, such as the number of lattice, lattice shapes, lattice spacing, and relative volume fraction. Another difficulty in using this PBG circuit is caused by the radiation from the periodic etched defects.

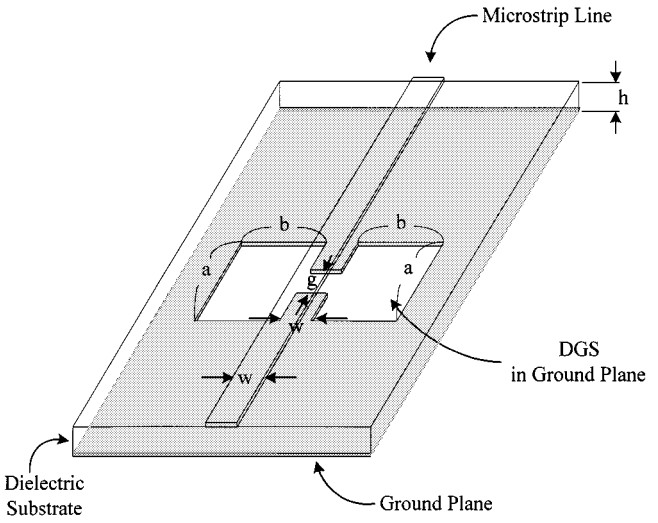

Fig. 1. Three-dimensional view of the proposed DGS unit section, which is etched in the ground plane of a microstrip line.

In this paper, a new etched lattice shape for the microstrip is proposed as a unit DGS. An etched defect in ground plane disturbs the shield current distribution in the ground plane. This disturbance can change characteristics of a transmission line such as line capacitance and inductance. The proposed DGS consists of narrow and wide etched areas in backside metallic ground plane as shown in Fig. 1, which give rise to increasing the effective capacitance and inductance of a transmission line, respectively. Thus, an *LC* equivalent circuit can represent the proposed unit DGS circuit. The effects of physical dimensions of the proposed DGS on these equivalent-circuit parameters are described. It is the purpose of this paper to show a potential for applying the proposed DGS to practical circuits. To design a circuit with the proposed DGS section, the equivalent circuit and parameters for the DGS section should be extracted. In this paper, the equivalent circuit of the proposed DGS unit section is derived by using the field analysis method. The equivalent-circuit parameters are extracted based on the circuit analysis theory. By employing the extracted parameters and the circuit analysis theory, the bandgap effect for the provided DGS section can be explained. Three-pole low-pass filters are designed by using the proposed DGS sections and the equivalent circuit. A DGS section can be performed as a series element of

Manuscript received July 14, 1999.

D. Ahn, J.-S. Park, and C.-S. Kim are with the School of Electrical and Electronic Engineering, Soonchunhyang University, Asan 336-745, Korea.

J. Kim, Y. Qian, and T. Itoh are with the Electrical Engineering Department, University of California at Los Angeles, Los Angeles, CA 90024 USA.

Publisher Item Identifier S 0018-9480(01)00025-4.

a low-pass filter. The shunt capacitance for low-pass filters will be implemented by employing the open stub.

The low-pass filter using the DGS circuit has a number of attractive features, which include the following.

1) The structure is very simple
2) The stopband is very wide and more deeper than that of a conventional low-pass filter.
3) The insertion loss is very low.
4) Extremely small element values for implementation of low-pass filter can be realized.

The validity of the modeling method for the proposed DGS unit section and the design method for the low-pass filter is verified by experiments.

II. Frequency Characteristics of DGS

Fig. 1 shows the etched lattice shape of the proposed DGS section, which is located on the backside metallic ground plane. The proposed DGS unit section can provide cutoff frequency and attenuation pole in some frequency without any periodic array of DGS. In order to investigate the frequency characteristics of the DGS section, we simulated the DGS unit section by Ansoft HFSS V.6.0. The simulation results show that one-pole low-pass filter characteristics, as expected. Existing of the cutoff frequency means that employing the DGS section increases the effective permittivity so that the effective inductance of a microstrip is also increased. The cutoff frequency is mainly dependent to the etched square area in ground plane. There is also attenuation pole location, which is due to the etched gap distance. Actually, it is well known that an attenuation pole can be generated by combination of the inductance and capacitance elements. Thus, to explain the frequency characteristic of the proposed DGS section, the presence of a capacitance factor should be needed. The etched gap area, which is placed under a conductor line, as shown in Fig. 1, provides the parallel capacitance with effective line inductance. Thus, the proposed DGS section is fully described by two parameters: the etched lattice dimension and gap distance. We showed the influences of these two parameters on frequency characteristics of a microstrip by simulations. All simulations were carried out by three-dimensional (3-D) HFSS.

A. Influence of the Square Lattice Dimension

The linewidth was chosen to be the characteristic impedance of 50-Ω microstrip line for simulations. Three DGS unit circuits without any period were simulated with the different dimension. In order to investigate the influence of the square lattice dimension, the etched gap, which is related with the gap capacitance, was kept constant to 0.2 mm for all three cases and the etched square area was varied. The substrate with 62-mil thick and a dielectric constant of ten was used for all simulations. The simulation results are illustrated in Fig. 2. From Fig. 2, one clearly observes that employing the proposed etched lattice increases the series inductance to the microstrip line. This effective series inductance introduces the cutoff characteristic at certain frequency. As the etched area of the unit lattice is increased, the effective series inductance increases, and increasing the series inductance gives rise to a lower cutoff frequency, as seen in Fig. 2. There are attenuation poles in simulation results on the etched unit lattices. These attenuation poles can be explained by parallel capacitance with the series inductance, as was explained previously. This capacitance depends on the etched gap below the conductor line, which is noted as g in Fig. 1. The capacitance values are identical for all cases due to the identical gap distance. However, the attenuation pole location, which corresponds to the resonance frequency of the parallel *LC* circuit, also becomes lower because as the series inductance increases, the resonance frequency of the equivalent parallel *LC* circuit decreases.

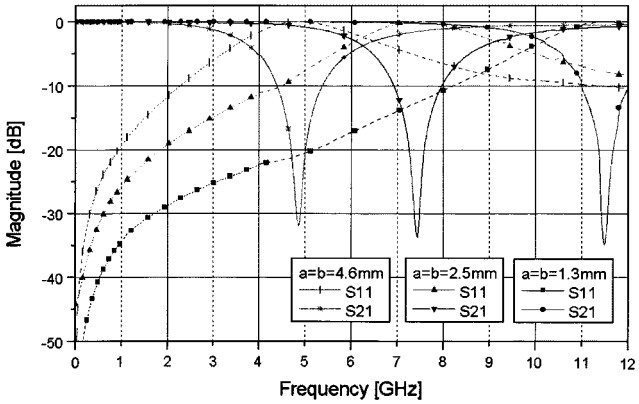

Fig. 2. Simulated S-parameters for the proposed DGS unit lattices. The gap distance g is 0.2 mm for all cases. The lattice dimension is $a = b = 1.3$ mm, $a = b = 2.5$ mm, and $a = b = 4.6$ mm, respectively. The substrate with 62-mil-thick and a dielectric constant of ten was used for all cases.

B. Influence of the Gap Distance

We now investigate the influence of the etched gap distance. The lattice dimension $a \times b$ was kept constant to 2.5 mm $\times$ 2.5 mm for all three cases and the etched gap distance was varied. The simulation results are shown in Fig. 3. Due to the constant lattice dimensions, we can expect that the effective series inductances are also constant for all cases. Unlike the influence of lattice dimension, there is no change in cutoff frequency despite the variation of the gap distance. This means that the gap distance does not affect the effective series inductance of a microstrip. Variation of the effective capacitance only affects the attenuation pole location, as seen in Fig. 3. As the etched gap distance increases, the effective capacitance decreases so that the attenuation pole location moves up to higher frequency. Simulation results seen in Fig. 2 and Fig. 3 pertinently show the influences of the proposed DGS section on frequency characteristics.

This equivalent circuit of the proposed DGS unit can explain the bandgap effect. The series inductance due to the DGS section increases the reactance of a microstrip with the increasing of the frequency. Thus, the rejection of the certain frequency range can be started. The parallel capacitance with the series inductance provides the attenuation pole location, which is the resonance frequency of the parallel *LC* resonator. However, as the operating frequency increases, the reactance of the capacitance decreases. Thus, the bandgap between the propagating frequency bands can be occurred.

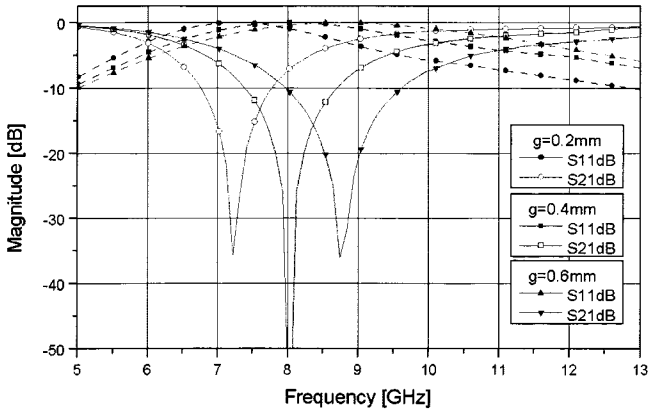

Fig. 3. Simulated S-parameters for the proposed DGS unit lattices. The lattice dimension is $a = b = 2.5$ mm for all cases. The gap distance is $g = 0.2$ mm, $g = 0.4$ mm, and $g = 0.6$ mm, respectively. The substrate with 62-mil-thick and a dielectric constant of ten was used for all cases.

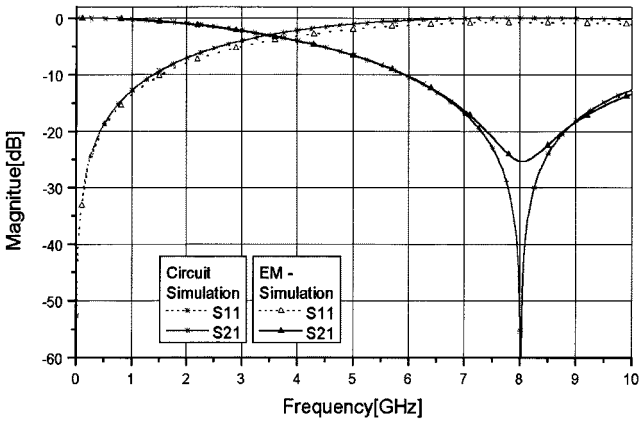

Fig. 4. Simulation results for proposed DGS unit section. The lattice dimension is $a = b = 5$ mm. The gap distance is $g = 0.5$ mm. The substrate with 31-mil-thick and a dielectric constant ε_r of 2.2 was used for simulation.

III. Modeling and Parameter Extraction

In the previous section, we have shown that the parallel *LC* circuit can represent the equivalent circuit of the proposed DGS section. Furthermore, effects of the proposed DGS parameters on the frequency characteristics have been investigated. From a practical point-of-view, the DGS section can serve as replacements for a parallel *LC* resonator circuit in many applications. To apply the proposed DGS section to a practical circuit design example, it is necessary to extract the equivalent circuit parameters. As an example of the parameter-extraction procedure, a, b, w, and g, which are dimensions of the DGS section shown in Fig. 1, have been chosen to be 5, 5, 2.4, and 0.5 mm, respectively. The substrate for simulations was an RT/Duroid 5880 with 31-mil-thick and a dielectric constant ε_r of 2.2. The simulation result is shown in Fig. 4 where solid lines are simulations by using 3-D HFSS. There is an attenuation pole near 8 GHz in the field simulation result. Fig. 4 shows the one-pole low-pass filter with an attenuation pole. In order to explain the cutoff and attenuation pole characteristic of the proposed DGS section simultaneously, the equivalent circuit should exhibit performances of low-pass and bandstop filter at the same time. Thus, the simple circuit shown in Fig. 5 can explain the phenomenon for the proposed DGS section.

The circuit parameters for the derived equivalent circuit can be extracted from the simulation result. The simulation result of the proposed DGS unit section can be matched to the one-pole Butterworth-type low-pass response, which has 3-dB cutoff frequency at 3.5 GHz. The series reactance value shown in Fig. 5 can be easily calculated by using the prototype element value of the one-pole Butterworth response. The prototype element value is given by various references. [14], [15] The parallel capacitance value for the given DGS unit dimension can be extracted from the attenuation pole location, which is parallel *LC* resonance frequency, and prototype low-pass filter characteristics by using the following procedures. The reactance value of the proposed DGS unit can be expressed as follows:

$$X_{\mathrm{LC}} = 1/\omega_o C\left(\frac{\omega_o}{\omega} - \frac{\omega}{\omega_o}\right) \tag{1}$$

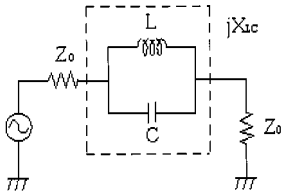

Fig. 5. Equivalent circuit of the proposed DGS circuit, where the dotted box shows the DGS section.

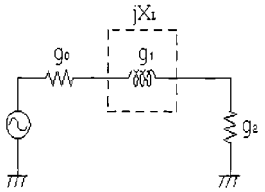

Fig. 6. Butterworth-type one-pole prototype low-pass filter circuit.

where ω_o is the resonance angular frequency of the parallel *LC* resonator, which is corresponding to attenuation pole location in Fig. 4. The series inductance of the Butterworth low-pass filter, shown in Fig. 6, can be derived as follows:

$$X_L = \omega' \cdot Z_o g_1 \tag{2}$$

where ω' denotes the normalized angular frequency, Z_o denotes the scaled impedance level of the in/out terminated ports, and g_1 is given by the prototype value of the Butterworth-type low-pass filter. In order to have the low-pass filter characteristics, the equivalent circuit of proposed DGS unit section, shown in Fig. 5, should be equal to the prototype low-pass filter, shown in Fig. 6, at a certain frequency. The equality at the cutoff frequency of the low-pass filter is given by the following:

$$X_{\mathrm{LC}}|_{\omega=\omega_c} = X_L|_{\omega'=1}\,. \tag{3}$$

From above equality, the series capacitance C of the equivalent circuit, shown in Fig. 5, can be obtained as follows:

$$C = \frac{\omega_c}{Z_o g_1} \cdot \frac{1}{\omega_o^2 - \omega_c^2}. \tag{4}$$

TABLE I
EXTRACTED EQUIVALENT-CIRCUIT PARAMETERS FOR THE PROPOSED UNIT DGS SECTION. THE GAP DISTANCE g IS 0.2 mm FOR ALL CASES

	DGS dimensions		
	$a = b$ = 1.3mm	$a = b$ = 2.5mm	$a = b$ = 4.6mm
Inductance (nH)	0.3675	0.865945	1.97725
Capacitance (pF)	0.51222	0.52845	0.537947
Cutoff Frequency (GHz)	10.15	6.085	3.62
Attenuation pole Location (GHz)	11.6	7.44	4.88

TABLE II
EXTRACTED EQUIVALENT-CIRCUIT PARAMETERS FOR THE PROPOSED UNIT DGS SECTION. THE LATTICE DIMENSION IS $a = b = 2.5$ mm FOR ALL CASES

	DGS dimension		
	g =0.2mm	g =0.4mm	g =0.6mm
Inductance (nH)	0.81051	0.90712	0.96825
Capacitance (pF)	0.60286	0.43306	0.34247
Cutoff Frequency (GHz)	6	6.4	6.72
Attenuation pole Location (GHz)	7.2	8.03	8.74

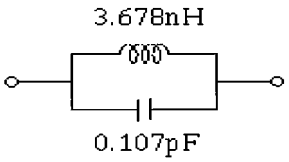

Fig. 7. Extracted equivalent-circuit parameters of the proposed DGS unit section, which has $a = b = 5$ mm, $w = 2.4$ mm, and $g = 0.5$ mm, respectively. The substrate with 31-mil-thick and a dielectric constant ε_r of 2.2 was used for simulation.

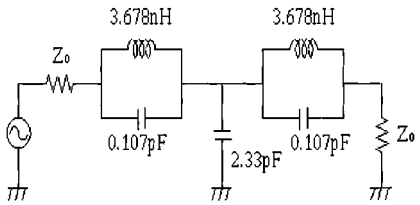

Fig. 8. Three-pole lumped low-pass filter with the equivalent circuits of a DGS unit section. The cutoff frequency is 1.3 GHz with 0.01-dB ripple level.

Once the capacitance value of the equivalent circuit is extracted, the series equivalent inductance for the given DGS unit section can be calculated by the following:

$$L = \frac{1}{4\pi^2 f_o^2 \cdot C} \tag{5}$$

where f_o is the frequency of the attenuation pole location and C is the extracted series capacitance value. Therefore, we can obtain each equivalent-circuit parameters by using (4) and (5), as shown in Fig. 7 [16]. Tables I and II show the extracted equivalent-circuit parameters for the proposed DGS unit sections, which are simulated in Figs. 2 and 3.

The equivalent-circuit simulation result using the obtained equivalent-circuit parameters is shown in Fig. 4 for comparison with the field calculated result. As show in Fig. 4, the equivalent-circuit simulation result shows excellent agreement with field calculations. Thus, the derived equivalent circuit and parameters for the proposed DGS section can be directly adapted to design a practical circuit. In the following section, we will demonstrate an example for low-pass filter design with the derived equivalent circuit and parameters.

IV. LOW-PASS FILTER DESIGN AND MEASUREMENTS

In order to show the validity of the equivalent circuit and extracted parameters for the proposed DGS unit section, three-pole low-pass filters with attenuation pole were designed by employing the proposed DGS unit structure at the cutoff frequency of a 1.3-GHz with 0.01-dB ripple level. Fig. 8 shows the lumped low-pass filter circuit with the equivalent circuit for DGS unit structure. The lumped low-pass filter circuit can be easily obtained from the prototype low-pass element values by proper frequency and impedance scaling. The parallel capacitance in a lumped low-pass filter can be realized by using the parallel open stub. The open stubs are realized with a T-junction structure and cross-junction structure, respectively. Fig. 9 shows a schematic of the designed low-pass filters with the proposed

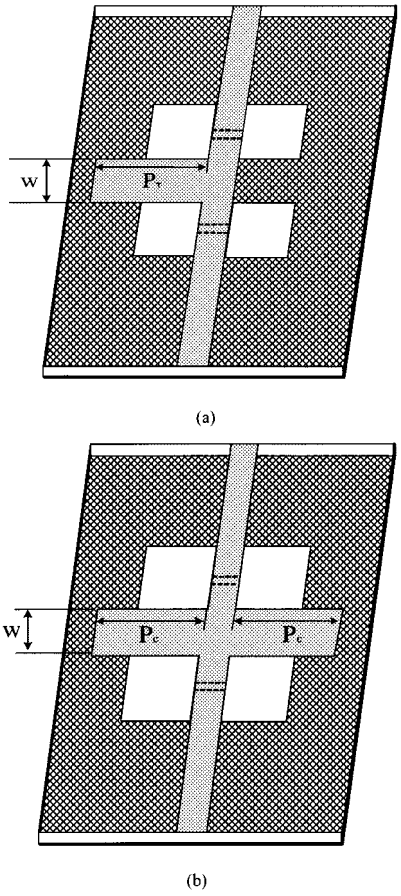

Fig. 9. Schematics of designed low-pass filters with the proposed DGS unit sections. (a) T-junction opened stub for parallel capacitance where the stub width w and length P_T are 5 and 10 mm, respectively. (b) Cross-junction opened stub for parallel capacitance where the stub width w and length P_C are 5 and 6 mm, respectively.

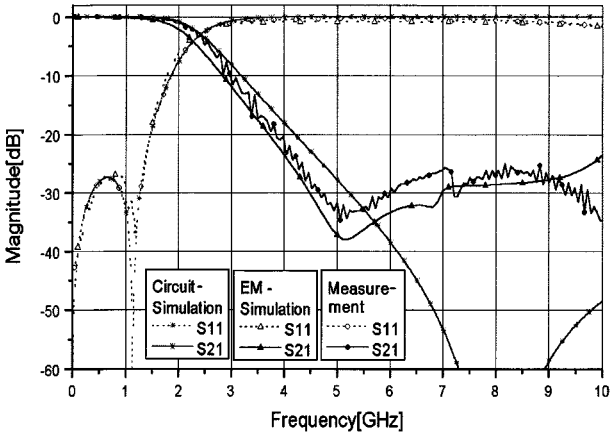

Fig. 10. Measured results for the fabricated DGS low-pass filter using the T-junction-type open stub with simulated data of a low-pass filter for comparison.

DGS sections. To implement the high-impedance inductance with a conventional microstrip, the conductor width becomes narrow. This is a limitation to use a microstrip low-pass filter configuration for high-power applications. By employing the proposed DGS sections, extremely small element values for implementation of a low-pass filter can be realized. Furthermore,

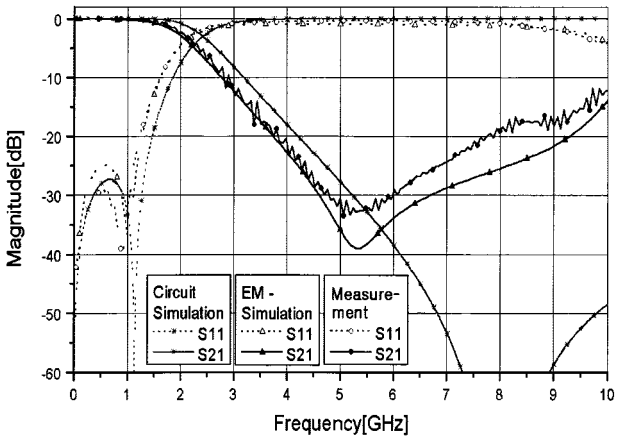

Fig. 11. Measured results for the fabricated DGS low-pass filter using the cross-junction-type open stub with the simulated data of a low-pass filter for comparison.

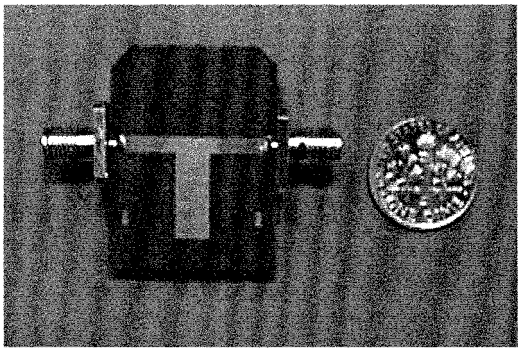

Fig. 12. Fabricated DGS low-pass filter with T-junction-type open stub. (a) Top view. (b) Bottom view.

the high-impedance inductance sections were realized by using DGS sections with a conductor width corresponding to a 50-Ω microstrip so that it can be expected that for DGS low-pass filters improve the power-handling capability.

Fig. 10 shows measured results for the fabricated DGS low-pass filter using the T-junction-type open stub with simulated data of a low-pass filter for comparison. Furthermore, Fig. 11 shows the comparison between measured results for the fabricated DGS low-pass filter with the cross-junction-type open stub and simulated data. Measurements and field calculations were carried out with absorbing boundary circumstance. Thus, these measurements and field calculations

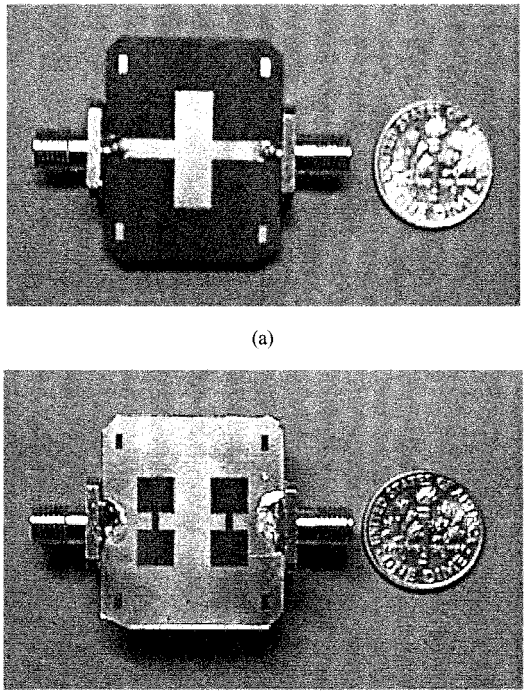

(a) (b)

Fig. 13. Fabricated DGS low-pass filter with cross-junction-type open stub. (a) Top view. (b) Bottom view.

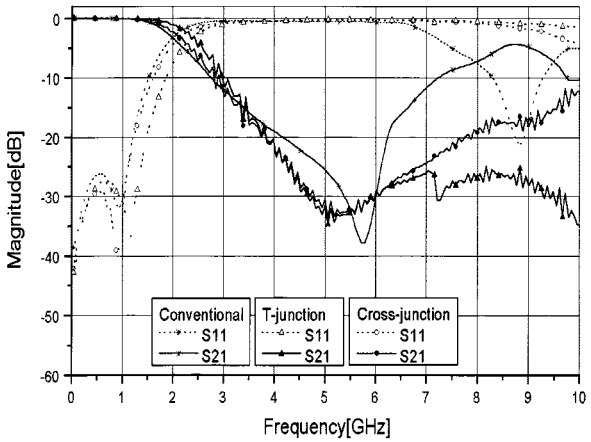

Fig. 14. Comparison of measured results for the fabricated DGS low-pass filters with the T-junction, cross-junction-type open stub, and conventional low-pass filter.

show differences with circuit simulated data in stopband due to radiation at DGS sections. Employing a metallic boundary for measurements and field calculations might show the improved stopband calculation. Figs. 12 and 13 show photographs of the fabricated low-pass filters with DGS section. The fabricated low-pass filters with the proposed DGS sections show relatively very simple configurations. To show the improved stopband characteristics of the DGS low-pass filters, we designed conventional low-pass filters with the same design specifications. Fig. 14 shows experimental results for the fabricated DGS low-pass filters using the T- and cross-junction-type open stub with the measured data of conventional low-pass filters as references. The attenuation characteristics for fabricated DGS low-pass filters show more than 20-dB filters up to 8 GHz. As can be seen, harmonic responses of conventional microstrip low-pass filters were started near 6 GHz. On the other hand, the DGS low-pass filters have relatively wider and deeper stopband characteristics than those of conventional low-pass filters. The measured insertion and return losses are less than 0.15 and 20 dB for all DGS low-pass filters, respectively. The measured data for fabricated DGS low-pass filters shows very low-level insertion and radiation loss, which could be generated by DGS, at the passband frequency range. The validity of the modeling method for the proposed DGS unit section and the design method for the low-pass filter is verified by experiments.

V. Conclusions

In this paper, the new DGS unit section and its equivalent circuit have been proposed. By using a simple circuit analysis method, the equivalent-circuit parameter extraction method for the proposed DGS unit section has also been derived. Furthermore, by employing the extracted parameters, the bandgap effect for the provided DGS section was explained based on circuit analysis theory. In order to show the validity of the proposed DGS structure and the derived equivalent circuit, the three-pole low-pass filters have been designed, fabricated, and then measured. Numerical simulations using 3-D HFSS show good agreement with experiments. The proposed DGS sections can realize small element values for implementation of a low-pass filter. Furthermore, the fabricated low-pass filter with the proposed DGS sections is expected to provide the improved the power-handling capability because that DGS section can implement the high impedance inductance line with broader conductor width than that of a conventional microstrip. The proposed DGS low-pass filters also have wider and deeper stopband characteristics than those of conventional low-pass filters. The measured data for fabricated DGS low-pass filters shows fairly good insertion-loss characteristic. This newly proposed DGS section and its equivalent circuit could also find various applications such as a bandpass filter, phase shifter, and multipole switch.

Acknowledgment

The authors sincerely appreciate Ansoft Korea's cooperation with our study and their support of simulation software.

References

[1] T. J. Ellis and G. M. Rebeiz, "MM-wave tapered slot antennas on micromachined photonic bandgap dielectrics," in *IEEE MTT-S Int. Microwave Symp. Dig.*, June 1996, pp. 1157–1160.

[2] M. M. Sigalas, R. Biswas, and K. M. Ho, "Theoretical study of dipole antennas on photonic–crystal substrate," *Microwave Opt. Technol. Lett.*, vol. 13, pp. 205–209, Nov. 1996.

[3] M. P. Kesler, J. G. Maloney, and B. L. Shirley, "Antenna design with the use of photonic bandgap material as all dielectric planar reflectors," *Microwave Opt. Technol. Lett.*, vol. 11, no. 4, pp. 169–174, Mar. 1996.

[4] V. Radisic, Y. Qian, R. Coccioli, and T. Itoh, "Novel 2-D photonic bandgap structure for microstrip lines," *IEEE Microwave Guide Wave Lett.*, vol. 8, pp. 69–71, Feb. 1998.

[5] E. Yablonovitch, "Photonic band-gap structures," *J. Opt. Soc. Amer. B, Opt. Phys.*, vol. 10, pp. 283–295, Feb. 1993.

[6] Y. Qian, F. R. Yang, and T. Itoh, "Characteristics of microstrip lines on a uniplanar compact PBG ground plane," in *Asia–Pacific Microwave Conf. Dig.*, Dec. 1998, pp. 589–592.

[7] Y. Qian and T. Itoh, "Planar periodic structures for microwave and millimeter wave circuit applications," in *IEEE MTT-S Int. Microwave Symp. Dig.*, June 1999, pp. 1533–1536.
[8] Y. Qian, V. Radisic, and T. Itoh, "Simulation and experiment of photonic bandgap structures for microstrip circuits," in *Proc. APMC'97*, pp. 585–588.
[9] V. Radisic, Y. Qian, and T. Itoh, "Broadband power amplifier using dielectric photonic bandgap structure," *IEEE Microwave Guide Wave Lett.*, vol. 8, pp. 13–14, Jan. 1998.
[10] ——, "Broad-band power amplifier integrated with slot antenna and novel harmonic tuning structure," in *IEEE MTT-S Int. Microwave Symp. Dig.*, June 1998, pp. 1895–1898.
[11] F. R. Yang, Y. Qian, R. Coccioli, and T. Itoh, "A novel low loss slow-wave microstrip structure," *IEEE Microwave Guide Wave Lett.*, vol. 8, pp. 372–374, Nov. 1998.
[12] K. P. Ma, K. Hirose, F. R. Yang, Y. Qian, and T. Itoh, "Realization of magnetic conducting surface using novel photonic bandgap structure," *Electron. Lett.*, vol. 34, pp. 2041–2042, Nov. 1998.
[13] F. R. Yang, K. P. Ma, Y. Qian, and T. Itoh, "A novel TEM waveguide using uniplanar compact photonic-bandgap (UC-PBG) structure," *IEEE Trans. Microwave Theory Tech.*, vol. 47, pp. 2092–2098, Nov. 1999.
[14] G. L. Matthaei, L. Young, and E. M. T. Jones, *Microwave Filters, Impedance Matching Networks and Coupling Structures*. Norwood, MA: Artech House, 1980, pp. 217–228.
[15] D. M. Pozar, *Microwave Engineering*. Reading, MA: Addison-Wesley, 1990, pp. 486–517.
[16] J. I. Park, C. S. Kim, J. Kim, J. S. Park, Y. Qian, D. Ahn, and T. Itoh, "Modeling of a photonic bandgap and its application for the low-pass filter design," in *APMC'99 Dig.*, pp. 331–334.

Dal Ahn (M'93) was born in Kimje, Korea, on October 15, 1961. He received the B.S., M.S., and Ph.D. degrees from Sogang University, Seoul, Korea, in 1984, 1986, and 1990, respectively, all in electronics.

From 1990 to 1992, he was with the Mobile Communications Division, Electronics and Telecommunications Research Institute (ETRI), Daejeon, Korea. Since 1992, he has been with the School of Electrical and Electronic Engineering, Soonchunhyang University, Asan, Korea, where he is currently an Associate Professor. He is also currently Chief of the RF and Microwave Component Research Center (RAMREC), Soonchunhyang University. He is also a technical consultant for Tel Wave Inc., Suwon, Korea. His current research interests include the design and application of passive and active components at radio and microwave frequencies, design of the RF front-end module for various handset system using LTCC technology, DGS circuit applications, and circuit modeling using a commercial electromagnetic analysis program. He is an Editor of the *Journal of Korea Electromagnetic Engineering Society*.

Jun-Seok Park (S'95–A'99) was born in Seoul, Korea, on August 12, 1969. He received the B.S. degree in electronic engineering, M.S. degree in electronic engineering, and Ph.D. degree from Kookmin University, Seoul, Korea, in 1991, 1993, and 1996, respectively.

In 1997, he joined the Department of Electrical Engineering, University of California at Los Angeles, as a Postdoctoral Researcher. In March 1998, he joined the Soonchunhyang University, Asan, Korea, as an Assistant Professor of electronic and electrical engineering. He is also currently a Senior Researcher at the RF and Microwave Component Research Center (RAMREC), Soonchunhyang University. His research interests include electromagnetic-field analysis and simulation, passive components, design of RF front-end modules for various handset systems using LTCC technology, DGS circuit applications, and RF active devices, as well as RF modules for Korea Cellular and PCS systems.

Chul-Soo Kim (S'99) was born in Kangwon, Korea, in 1969. He received the B.S. and M.S. degrees in electronic engineering from Soonchunhyang University, Asan, Korea, in 1996 and 1998, respectively, and is currently working toward the Ph.D. degree in electronic engineering at Soonchunhyang University.

His current research interests include passive components for wireless communications.

Juno Kim (S'93) was born in Seoul, Korea, in 1968. He received the B.S. and M.S. degrees in electrical engineering from Seoul National University, Seoul, Korea, in 1993 and 1995, respectively, and is currently working toward the Ph.D. degree in electrical engineering at the University of California at Los Angeles.

His current research interests include millimeter-wave wireless communication circuits using silicon devices.

Yongxi Qian (S'91–M'93) was born in Shanghai, China, in 1965. He received the B.E. degree from Tsinghua University, Beijing, China, in 1987, and the M.E. and Ph.D. degrees from the University of Electro-Communications, Tokyo, Japan, in 1990 and 1993, respectively, all in electrical engineering.

From 1993 to 1996, he was an Assistant Professor at the University of Electro-Communications. In April 1996, he joined the University of California at Los Angeles (UCLA), where he is currently an Assistant Research Engineer in the Electrical Engineering Department. He has performed research on various numerical techniques for microwave and millimeter-wave circuits and antennas, generation and transmission of picosecond electrical pulses, crosstalk problems in high-density monolithic microwave integrated circuits (MMICs), miniature circuits for mobile communications, and a 60-GHz millimeter-wave focal plane imaging array. He has authored or co-authored over 160 refereed journal and conference papers, two books, and several book chapters. His current research interests include broad-band planar antennas, smart antennas and arrays for wireless communications, high-efficiency microwave power amplifiers, RF interconnect for mixed-signal silicon MMICs, quasi-optical power-combining PBG structures, active integrated antennas for indoor local area networks (LANs), and high-power broad-band RF photonic devices for millimeter- and submillimeter-wave photomixing.

Dr. Qian was the recipient of the Japan Microwave Prize presented at the 1998 Asia–Pacific Microwave Conference and Best Student Paper Award (as co-author) presented at the 1999 29th European Microwave Conference.

Tatsuo Itoh (S'69–M'69–SM'74–F'82) received the Ph.D. degree in electrical engineering from the University of Illinois at Urbana-Champaign, in 1969.

From September 1966 to April 1976, he was with the Electrical Engineering Department, University of Illinois at Urbana-Champaign. From April 1976 to August 1977, he was a Senior Research Engineer in the Radio Physics Laboratory, SRI International, Menlo Park, CA. From August 1977 to June 1978, he was an Associate Professor at the University of Kentucky, Lexington. In July 1978, he joined the faculty at The University of Texas at Austin, where he became a Professor of electrical engineering in 1981 and Director of the Electrical Engineering Research Laboratory in 1984. During the summer of 1979, he was a Guest Researcher at AEG-Telefunken, Ulm, Germany. In September 1983, he was selected to hold the Hayden Head Centennial Professorship of Engineering at The University of Texas at Austin. In September 1984, he was appointed Associate Chairman for Research and Planning of the Electrical and Computer Engineering Department, The University of Texas at Austin. In January 1991, he joined the University of California at Los Angeles, as Professor of electrical engineering and Holder of the TRW Endowed Chair in Microwave and Millimeter Wave Electronics. He was an Honorary Visiting Professor at Nanjing Institute of Technology, Nanjing, China, and at the Japan Defense Academy. In April 1994, he became an Adjunct Research Officer for Communications Research Laboratory, Ministry of Post and Telecommunication, Japan. He currently holds a Visiting Professorship at The University of Leeds, Leeds, U.K., and is an External Examiner of the Graduate Program of City University of Hong Kong. He has authored or co–authored 265 journal publications, 515 refereed conference presentations, and 30 books/book chapters in the area of microwaves, millimeter-waves, antennas and numerical electromagnetics. He has also generated 43 Ph.D. students.

Dr. Itoh is a member of the Institute of Electronics and Communication Engineers of Japan, and Commissions B and D of USNC/URSI. He served as Editor-in-Chief of IEEE TRANSACTIONS ON MICROWAVE THEORY AND TECHNIQUES (1983–1985). He serves on the Administrative Committee of the IEEE MTT-S. He was Vice President of the IEEE MTT-S in 1989 and President in 1990. He was Editor-in-Chief of IEEE MICROWAVE AND GUIDED WAVE LETTERS from 1991 to 1994. He was elected as an Honorary Life Member of the IEEE MTT-S in 1994. He was the chairman of USNC/URSI Commission D (1988–1990), and chairman of Commission D of the International URSI (1993–1996). He is chair of the Long-Range Planning Committee of URSI. He serves on advisory boards and committees of a number of organizations. He has been the recipient of a number of awards, including the 1998 Shida Award presented by the Japanese Ministry of Post and Telecommunications and the 1998 Japan Microwave Prize.

射 频 和 天 线 设 计 培 训 课 程 推 荐

易迪拓培训(www.edatop.com)由数名来自于研发第一线的资深工程师发起成立，致力并专注于微波、射频、天线设计研发人才的培养；我们于 2006 年整合合并微波 EDA 网(www.mweda.com)，现已发展成为国内最大的微波射频和天线设计人才培养基地，成功推出多套微波射频以及天线设计经典培训课程和 ADS、HFSS 等专业软件使用培训课程，广受客户好评；并先后与人民邮电出版社、电子工业出版社合作出版了多本专业图书，帮助数万名工程师提升了专业技术能力。客户遍布中兴通讯、研通高频、埃威航电、国人通信等多家国内知名公司，以及台湾工业技术研究院、永业科技、全一电子等多家台湾地区企业。

易迪拓培训课程列表：http://www.edatop.com/peixun/rfe/129.html

射频工程师养成培训课程套装

该套装精选了射频专业基础培训课程、射频仿真设计培训课程和射频电路测量培训课程三个类别共 30 门视频培训课程和 3 本图书教材；旨在引领学员全面学习一个射频工程师需要熟悉、理解和掌握的专业知识和研发设计能力。通过套装的学习，能够让学员完全达到和胜任一个合格的射频工程师的要求…

课程网址：http://www.edatop.com/peixun/rfe/110.html

ADS 学习培训课程套装

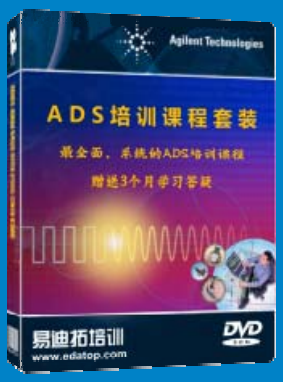

该套装是迄今国内最全面、最权威的 ADS 培训教程，共包含 10 门 ADS 学习培训课程。课程是由具有多年 ADS 使用经验的微波射频与通信系统设计领域资深专家讲解，并多结合设计实例，由浅入深、详细而又全面地讲解了 ADS 在微波射频电路设计、通信系统设计和电磁仿真设计方面的内容。能让您在最短的时间内学会使用 ADS，迅速提升个人技术能力，把 ADS 真正应用到实际研发工作中去，成为 ADS 设计专家...

课程网址： http://www.edatop.com/peixun/ads/13.html

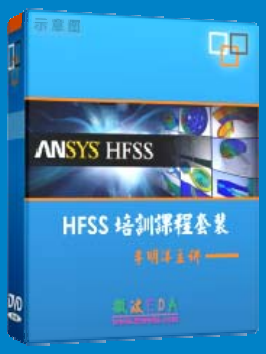

HFSS 学习培训课程套装

该套课程套装包含了本站全部 HFSS 培训课程，是迄今国内最全面、最专业的 HFSS 培训教程套装，可以帮助您从零开始，全面深入学习 HFSS 的各项功能和在多个方面的工程应用。购买套装，更可超值赠送 3 个月免费学习答疑，随时解答您学习过程中遇到的棘手问题，让您的 HFSS 学习更加轻松顺畅…

课程网址：http://www.edatop.com/peixun/hfss/11.html

CST 学习培训课程套装

该培训套装由易迪拓培训联合微波 EDA 网共同推出，是最全面、系统、专业的 CST 微波工作室培训课程套装，所有课程都由经验丰富的专家授课，视频教学，可以帮助您从零开始，全面系统地学习 CST 微波工作的各项功能及其在微波射频、天线设计等领域的设计应用。且购买该套装，还可超值赠送 3 个月免费学习答疑…

课程网址：http://www.edatop.com/peixun/cst/24.html

HFSS 天线设计培训课程套装

套装包含 6 门视频课程和 1 本图书，课程从基础讲起，内容由浅入深，理论介绍和实际操作讲解相结合，全面系统的讲解了 HFSS 天线设计的全过程。是国内最全面、最专业的 HFSS 天线设计课程，可以帮助您快速学习掌握如何使用 HFSS 设计天线，让天线设计不再难…

课程网址：http://www.edatop.com/peixun/hfss/122.html

13.56MHz NFC/RFID 线圈天线设计培训课程套装

套装包含 4 门视频培训课程，培训将 13.56MHz 线圈天线设计原理和仿真设计实践相结合，全面系统地讲解了 13.56MHz 线圈天线的工作原理、设计方法、设计考量以及使用 HFSS 和 CST 仿真分析线圈天线的具体操作，同时还介绍了 13.56MHz 线圈天线匹配电路的设计和调试。通过该套课程的学习，可以帮助您快速学习掌握 13.56MHz 线圈天线及其匹配电路的原理、设计和调试…

详情浏览：http://www.edatop.com/peixun/antenna/116.html

我们的课程优势：

※ 成立于 2004 年，10 多年丰富的行业经验，

※ 一直致力并专注于微波射频和天线设计工程师的培养，更了解该行业对人才的要求

※ 经验丰富的一线资深工程师讲授，结合实际工程案例，直观、实用、易学

联系我们：

※ 易迪拓培训官网：http://www.edatop.com

※ 微波 EDA 网：http://www.mweda.com

※ 官方淘宝店：http://shop36920890.taobao.com